Available online at www.sciencedirect.com
ScienceDirect
Journal of the European Ceramic Society 26 (2006) 3301–3306
www.elsevier.com/locate/jeurceramsoc

Erbium-doped LAS glass ceramics prepared by spark plasma sintering (SPS)

P. Riello [a,*], S. Bucella [a], L. Zamengo [a], U. Anselmi-Tamburini [b,d], R. Francini [c], S. Pietrantoni [c], Z.A. Munir [d]

[a] *Dipartimento di Chimica Fisica, Università di Venezia Ca' Foscari, Via Torino 155b, 30170 Venezia-Mestre, Italy*
[b] *Dipartimento di Chimica fisica, Universita' di Pavia, V.le Taramelli 16, 27100 Pavia, Italy*
[c] *Dipartimento di Fisica and Istituto Nazionale di Fisica della Materia, Università di Roma Tor Vergata, Via della Ricerca Scientifica 1, 00133 Roma, Italy*
[d] *Department of Chemical Engineering and Materials Science, University of California, Davis, USA*

Received 8 May 2005; received in revised form 21 July 2005; accepted 4 August 2005
Available online 3 October 2005

Abstract

Dense nanocrystalline glass ceramics of the Li_2O–Al_2O_3–SiO_2 (LAS) system were obtained by spark plasma sintering (SPS) of powders prepared by sol–gel method. The low thermal expansion LAS glass ceramic was chosen as host matrix for erbium ions. ZrO_2 was added both as a nucleating agent and as a possible good environment for the rare earth. The developed crystalline phases were analysed by X-ray diffraction (XRD) and the amorphous phase was quantified. Scanning and transmission electron microscopy (SEM, TEM) was used to investigate the microstructure. A different behaviour during the crystallisation process was observed between the sample prepared through the sintering of powders and the glass produced by the melting technique. A photoluminescence characterisation was also performed.
© 2005 Elsevier Ltd. All rights reserved.

Keywords: Sintering; Glass ceramics; Transition metal oxides; Optical properties; Spark plasma sintering; LAS

1. Introduction

Transparent glass ceramics have been investigated for optical applications such as solar collectors, up-conversion devices and laser media.[1] Some recent papers[2–7] have proposed some interesting applications of transparent glass-ceramics of various chemical compositions containing nano-sized crystalline phases doped with luminescent lanthanide ions. The goal is to obtain crystal-like optical properties in a composite material with macroscopic glass properties. Depending on the glass host and the crystal phase composition, it is possible to obtain materials with improved mechanical, thermal, electrical or optical properties. Some recent studies concern the luminescent properties of Er^{3+}-doped TiO_2 or ZrO_2 nanocrystals or glasses in which $Er_2Ti_2O_7$ and $ErPO_4$ nanocrystals[8–10] are developed after thermal treatment.

Luminescent oxide glass ceramics in the Li_2O–Al_2O_3–SiO_2 system could be extremely interesting because of the high thermal-mechanical strength, near zero thermal expansion and transparency.[11,12] Glass-ceramics in this group are usually produced by promoting the volume nucleation in melt-derived bulk. It is possible to obtain a large number of nuclei (up to 10^{17} nuclei/cm^3) by introducing ZrO_2, TiO_2, P_2O_5 or a mixture of them. In such a way a large number of nanocrystallites (5–20 nm), belonging to the nucleating phase (for example ZrO_2 or $ZrTiO_4$), is developed in the glassy matrix.

Alternative processes are based on the compaction and sintering of fine glass-melt or sol–gel-derived powders.[13–20] The sintering usually requires long treatment time and develops a crystalline coarse grain structure but it is possible to obtain full-density materials in the amorphous state if high heating rates are used.[16]

The glass composition studied in this work belongs to the LAS phase diagram (SiO_2 73 wt.%, Al_2O_3 23 wt.%, Li_2O 4 wt.%) known to lead to a transparent glass ceramic constituted of β-quartz solid solutions (75%) and a residual glass.

* Corresponding author.
E-mail address: riellop@unive.it (P. Riello).

0955-2219/$ – see front matter © 2005 Elsevier Ltd. All rights reserved.
doi:10.1016/j.jeurceramsoc.2005.08.003

In the present work LAS glass ceramics containing small amounts of zirconium oxide are chosen as host matrix for erbium ions. ZrO_2 was added not only as a nucleating agent but also because it is an excellent host for the luminescence ions thanks to its optical transparency, hardness, high chemical and photochemical stability, high refractive index and low phonon energy.[21] In fact, in order to reduce non-radiative transitions generally due to multi-phonon relaxations, it is necessary to surround the active ions by a matrix that possesses low vibrational energies.

The powders obtained by the sol–gel route were sintered by spark plasma sintering (SPS)[22–24] which allows to achieve higher densities at lower temperatures and in a very short time with respect to other approaches (i.e. traditional hot pressing), even with materials that are difficult to sinter uniformly (e.g. ZrO_2-based materials).

In this paper, we compared Er-doped LAS glass ceramic materials obtained by SPS with those prepared by melting. To the best of our knowledge this is the first paper that verifies the applicability of SPS on LAS glass ceramic.

2. Experimental procedure

2.1. Sample preparation

The samples prepared by the sol–gel and melting techniques have the molar composition given in Table 1. The powders were prepared by the aqueous sol–gel route. The starting materials were tetraethoxy silane (TEOS) (98%, Aldrich), lithium carbonate (99%, Aldrich), zirconium oxychloride octahydrate (98%, Aldrich), aluminum nitrate nonahydrate (98%, Aldrich) and erbium chloride hexahydrate (99.9%, Aldrich). Freshly prepared aluminum and zirconium hydroxides, obtained by the addition of 30% ammonia to the salt water solutions, were reacted with formic acid. Lithium formate was prepared from lithium carbonate. Erbium was directly introduced as the chloride salt and TEOS was lastly added to the water solution containing the right amount of metal ions. The sol was heated at 70 °C until gelation took place and the resulting powder was annealed in air for 24 h at 490 °C.

The glass was melted in an electrically heated furnace at 1660 °C within a platinum crucible. Nucleation of the as-quenched glass was attempted in a range of temperature between 750 and 1000 °C.

2.2. Spark plasma sintering

Sintering was performed in an SPS Dr.Sinter 1050 unit (Sumitomo Coal Mining Co.) using cylindrical graphite dies. A gas pressure of 10 Pa was maintained in the apparatus during the sintering process. The electrical power was delivered by the SPS apparatus through the die in rapid pulses, 3 ms in length. Each pulse has a maximum voltage in the range 0–10 V and a peak current of several thousand amperes. A pulse pattern of 12:2 (meaning 12 pulses on and 2 off) was used. A uniaxial pressure ranging between 35 and 53 MPa was applied throughout the entire densification process. Densification temperatures between 840 and 900 °C were used. The sample was heated up to the desired temperature with a rate of 200 °C/min. The sintered samples were disk shaped with a diameter of 19 mm and thickness of 2–3 mm.

Table 1
Molar composition of the SPS and melted samples

	SiO_2	Al_2O_3	Li_2O	ZrO_2	Er_2O_3
SPS	77.0	13.86	7.71	1.04	0.39
Melted[a]	76.7	13.80	7.93	1.02	0.55

[a] The sample contains 4 mol% of BaO, ZnO, As_2O_3, Na_2O, K_2O, MgO.

2.3. Physical characterisation

The XRD patterns were collected at 295 K, with a step size of 0.05° in the preset-time mode (10 s). In order to improve the signal to noise ratio, at least three runs were measured. Philips diffractometers, equipped with a focusing graphite monochromator on the diffracted beam and with a proportional counter with an electronic pulse height discrimination was used. Moreover, a divergence slit of 0.5°, a receiving slit of 0.2 mm., an anti-scatter slit of 0.5° and Fe-filtered Co Kα radiation were employed.

The quantitative phase analysis by X-ray diffraction was performed using the Rietveld method (DBWS9600 computer program written by Sakthivel and Young modified by Riello et al.).[25,26] This method was previously successfully applied to the study of crystallization of LAS glass ceramic materials.[12]

The procedure allows the quantitative analysis of the crystalline phases, even if an amorphous matrix is present, without adding any internal standard to the sample. The quantification of the different phases is based on the assumption that the whole chemical composition of the sample does not change during the treatments.

Transmission electron microscopy (TEM) images were taken at 300 kV with a Jeol 3010 instrument with an ultra-high resolution (UHR) pole-piece (0.17 nm point resolution), equipped with a Gatan slow-scan CCD camera (Mod. 794) and an Oxford Instrument EDS microanalysis detector (Mod. 6636). The powdered samples were dispersed in isopropyl alcohol solution by sonication for about 5 min and than deposited onto a holey carbon film.

Scanning electron microscopy (SEM) images were taken with a Jeol (Tokyo, Japan) JSM 5600 LV (low vacuum) microscope equipped with an Oxford Instruments (Oxford, England) 6587 energy dispersive spectroscopy (EDS) microanalysis detector. Samples were coated with an Au thin film in order to avoid charging effects.

For the infrared (IR) spectroscopic investigations all measurements were performed at room temperature by exciting the erbium ions at 980 nm using a continuous wave InGaAsP laser diode. The maximum laser power was about 1 W, but for stable operation a power of 400 mW was chosen. The laser beam was weakly focused on the sample to a spot of approximately 1 mm^2, corresponding to a power density of about 40 W/cm^2. The luminescence from the sample was collected and analysed

by a 30 cm focal length monochromator and detected with a cooled germanium detector.

Vickers microhardness measurements of glass ceramic tiles were made with an indenter (Galileo microscan OD). A load of 300 g for 30 s was used to indent the surfaces.

3. Results and discussion

Three sintering conditions characterized by different final temperature and pressure were used during the densification process: SPS1 850 °C 35 MPa 2 min; SPS2 840 °C 53 MPa 5 min; SPS3 900 °C 53 MPa 5 min.

Fig. 1 shows the XRD patterns of the sample prepared by sol–gel and sintered according to the conditions listed above. Only SPS3 achieved a marked crystallization while SPS1 and SPS2 are completely or almost completely amorphous. The XRD analysis, see inset in Fig. 1, shows that the crystalline portion is mainly constituted of β-eucryptite/β-quartz s.s. and a cubic-stabilised zirconia phase. Concerning the latter one only the formation of a ZrO_2–Er_2O_3 s.s. can explain the obtained cell parameter $a = 5.153$ Å due to the presence of a cation larger than Zr^{4+}. In order to establish the composition of the latter phase we compared the calculated lattice parameter with those of $Er_{0.2}Zr_{0.8}O_{1.9}$ ($a = 5.145$ Å, ICSD 62469) and $Er_{0.5}Zr_{0.5}O_{1.75}$ ($a = 5.190$ Å, ICSD 62452). Assuming a linear relation between the composition and the lattice parameter of the cubic cell we can estimate that in SPS3 the 30% of the introduced Er_2O_3 forms a solid solution with the ZrO_2 with the composition $Er_{0.25}Zr_{0.75}O_{1.875}$, while the remaining 70% is obviously in the amorphous or/and in the LAS phases. Table 2. reports the phase composition of the SPS samples obtained by using the cited Rietveld analysis.

Table 2
Relative density and phase composition of the SPS samples

	SPS1	SPS2	SPS3
Relative density (%)	99	96	96
Amorphous (wt.%)	100	99	55
β-Eucryptite/β-quartz s.s (wt.%).		1	39
β-Spodumene (wt.%)	–	–	2
$Er_{0.25}Zr_{0.75}O_{1.875}$ (wt.%)	–	–	2
Mullite (wt.%)	–	–	2

In Fig. 2A a TEM micrograph of SPS3 is reported. The dark particles, as confirmed by the EDX analysis (Fig. 3), are the ZrO_2–Er_2O_3 s.s. The crystallite size, obtained by the Scherrer equation, is 10 nm in agreement with the value obtained by TEM. The nuclei concentration,[12] $1.2 \times 10^{16}/cm^3$, is evaluated by knowing the density of SPS3, 2.48 g/cm^3. This value is very close to the density of the glass obtained by melting (2.50 g/cm^3) considered as the theoretical one, while the density of the SPS1 and SPS2 is only 96% of the full density. The average Vickers microhardness of SPS3 and the glass obtained by melting are 6.76 and 7.1 Gpa, respectively.

The β-quartz/β-eucryptite s.s. composition is $[SiO_2]_{0.83}[Al_2O_3{\cdot}Li_2O{\cdot}2SiO_2]_{0.17}$ obtained by the refined lattice parameters.[27] The crystallite size of this phase is 33 nm, a value that is 1–2 order of magnitude lower than the crystallite sizes reported in the literature for analogous sintered materials.

The three SPS samples are translucent. It is well known that good transparency requires low optical scattering, satisfied when

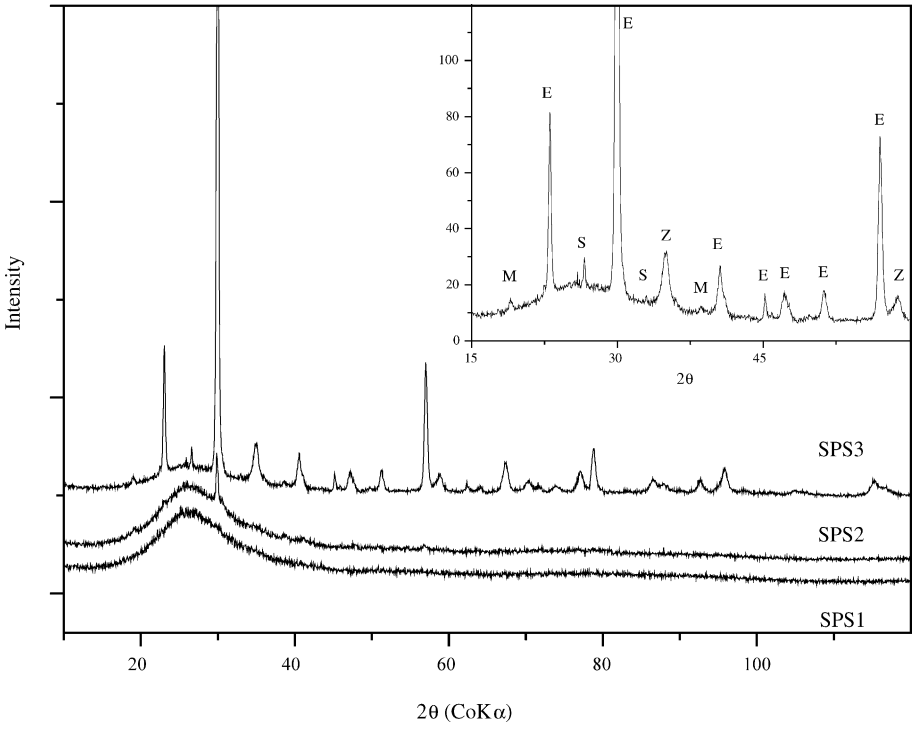

Fig. 1. XRD patterns of LAS SPS. Inset: magnification of SPS3 pattern. β-eucryptite/β-quartz s.s. (E); β-spodumene (S); mullite (M); $Er_{0.25}Zr_{0.75}O_{1.875}$ (Z).

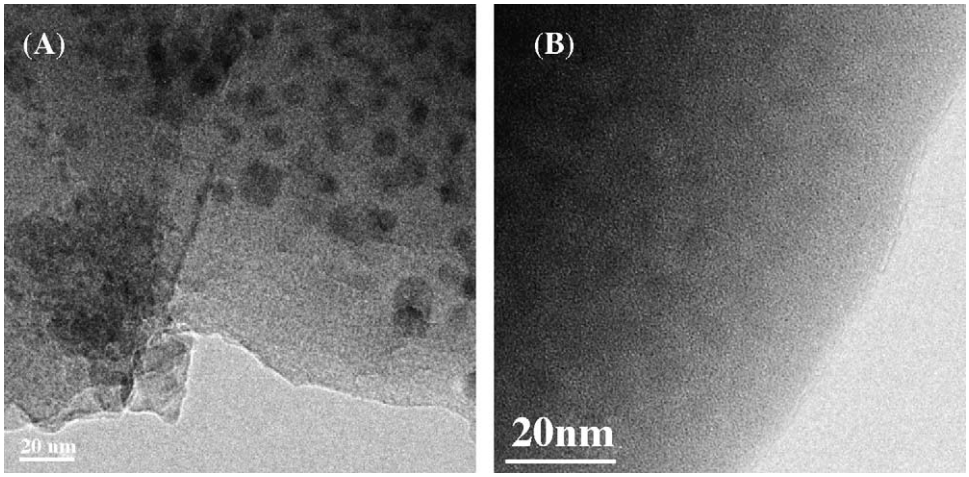

Fig. 2. TEM micrograph of SPS3 (A) and SPS2 (B).

the crystalline phases and the residual glass have very similar refraction indexes and when crystal sizes are much smaller than the wavelength of light. Even if these criteria are satisfied in our samples, the lack of transparency could be ascribed to the porosity. It is known, in fact, that only if the residual porosity is less than few ppm (perhaps 100 ppm) transparency is reached and, to confirm the latter hypothesis, the SEM image of the sample SPS3 is shown in Fig. 4.

Thus, in order to further decrease the porosity other SPS conditions must be explored.

Fig. 5 shows the IR emission spectra of the SPS samples. In the three cases the lineshape is identical, with a single peak at 1530 nm. The emission intensity decreases with the development of the crystalline phases (SPS3 is about six times lower than SPS1) because a large fraction of erbium (30 wt.%) moved to the zirconate phase and its concentration became high enough to give the quenching phenomenon. This effect can also explain the reduced emission intensity observed in SPS2 even if only 1 wt.%

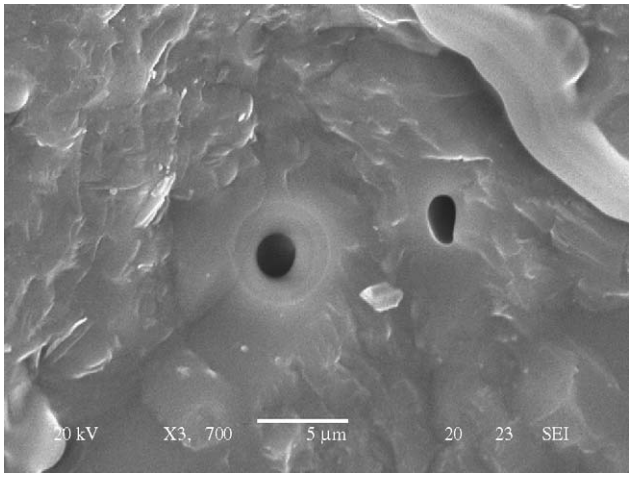

Fig. 4. SEM micrograph of SPS3 showing the residual porosity.

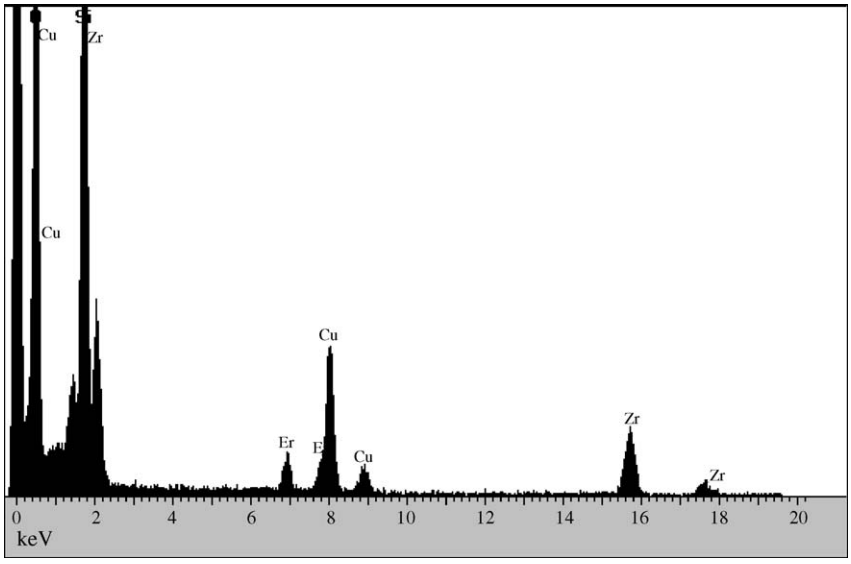

Fig. 3. EDX analysis of the particles in micrographes of SPS3 (Fig. 2A.)

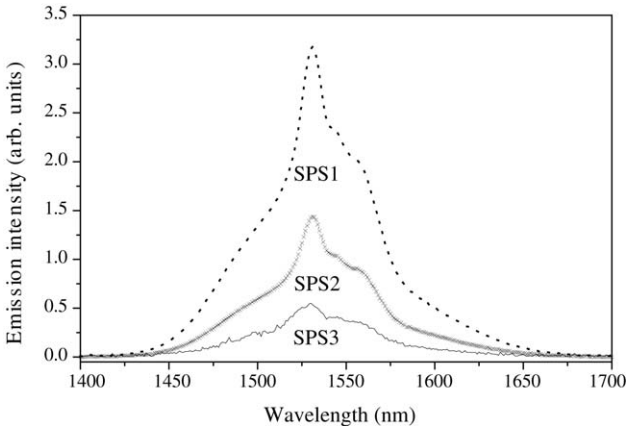

Fig. 5. IR emission spectra of Er^{3+} doped LAS SPS glass ceramics.

of β-eucriptyte crystallized. In fact, even if X-ray diffraction does not show any crystallization of the Er-rich zirconate phase, the TEM image of the SPS2 sample, reported in Fig. 2B, shows its incipient phase separation.

These results on one hand confirm the possibility of draining the rare earth from the silica rich matrix into the good environment provided by ZrO_2. On the other hand they suggest that one should increase the ZrO_2/Er_2O_3 ratio in order to reduce the erbium concentration in the ZrO_2 phase.

The samples obtained by sol–gel were also compared with glasses prepared by the melting technique. Despite the high temperature of the nucleation treatments (ranging from 750 to 1000 °C) the latter samples always showed amorphous like X-ray diffraction patterns: the nucleating agent ZrO_2 did not precipitate and no crystalline phase developed. This fact was also confirmed by small angle X-ray scattering which did not show any appreciable demixing of phases with different electron densities.

The different nucleation and crystallization behaviour of the sintered sample with respect to the glass obtained by melting can be explained considering the different microstructure: thanks to the high defect concentration on the surface of the sintered powders more suitable conditions for nucleation and crystallization are achieved.

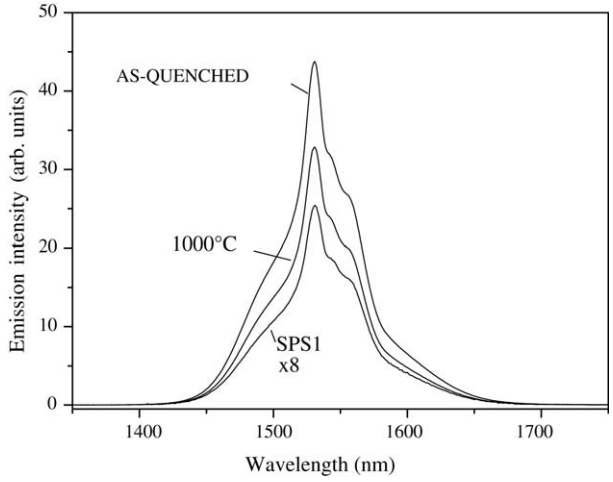

Fig. 6. IR emission spectra of LAS-Er-Zr samples prepared by melting.

It is interesting to observe that also the IR emission spectra of the glass samples have a behaviour analogous to the sintered ones (Fig. 6). The lineshape of the IR spectra is the same for all the samples (the as-quenched sample, the one treated at 1000 °C and the sintered one (SPS1)), but the emission intensity is higher for the as-quenched sample with respect to the one treated at 1000 °C for 24 h. It is worth noticing that the luminescence measurements show up the clustering of Er^{3+} ions, extremely sensitive to concentration quenching, even when diffraction-based techniques and TEM analysis were not able to put in evidence the incipient phase separation.

4. Conclusions

Monodispersed Erbium-stabilized zirconia nanoparticles (10 nm) were successfully developed from a LAS glass ceramic matrix through Spark Plasma Sintering of powders prepared by the sol–gel method. Completely amorphous samples or with 45 wt.% of crystalline phases can be obtained by choosing different conditions of temperature and pressure in the densification process. Although the sintered samples were not transparent, density and hardness of the most crystalline sample are very close to the values of the glass obtained by melting while for the amorphous (or near amorphous) samples the density is 96% of the theoretical one.

In the most crystalline sample the erbia-zirconia solid solution has cubic fluorite structure with composition $Er_{0.25}Zr_{0.75}O_{1.875}$. The erbium crystallized into the latter phase is 30 wt.% of the introduced erbium oxide.

The optical characterisation confirms the structural investigation showing a decrease of IR emission corresponding to the segregation of the erbium ions into the crystalline phases.

The lack of transparency of the most crystalline sample might be due to a residual porosity.

The nucleation of an Er_2O_3–ZrO_2–LAS glass prepared by melting in the range of temperature between 750 and 1000 °C failed since the nucleating agent ZrO_2 did not precipitate and no crystalline phase developed even at the highest temperature. The only difference was observed in the IR emission intensity showing that the as-quenched sample has an intensity higher than that one of the sample treated at 1000 °C probably due to the incipient Er^{3+} ions segregation.

Acknowledgements

The financial support from MURST (COFIN-2002) and INFM is gratefully acknowledged.

References

1. Malyarevich, A. M., Denisov, I. A., Volk, Y. V., Yumashev, K. V., Dymshits, O. S. and Zhilin, A. A., Nanosized glass-ceramics doped with transition metal ions: nonlinear spectroscopy and possible laser applications. *J. Alloy Comp.*, 2002, **341**(1–2), 247–250.
2. Auzel, F., Lipinska-Kalita, K. E. and Santa-Cruz, P., A new Er3+-doped vitreous fluoride amplification medium with crystal-like cross-sections

and reduced inhomogeneuous line width. *Opt. Mater.*, 1996, **5**, 75–78.
3. Mortier, M. and Auzel, F., Rare-earth doped transparent glass-ceramics with high cross-sections. *J. Non-Cyst. Solids*, 1999, **256/257**, 361–365.
4. Mortier, M., Monteville, A., Patriarche, G., Mazé, G. and Auzel, F., New progresses in transparent rare-earth doped glass-ceramics. *Opt. Mater.*, 2001, **16**, 255–267.
5. Dymnikov, A. A., Dymshits, O. S., Zhilin, A. A., Savostjanov, V. A. and Chuvaeva, T. I., The structure of luminescence centers in neodymium in glasses and trasparent glass-ceramics of the Li_2O–Al_2O_3–SiO_2 system. *J. Non-Cyst. Solids*, 1996, **196**, 67–72.
6. Kang, U., Chuvaeva, T. I., Onushchenko, A. A., Shashkin, A. V., Zhilin, A. A., Kim, H.-J. and Chang, Y.-G., Radiative properties of Nd-doped transparent glass-ceramics in the lithium aluminosilicate system. *J. Non-Cyst. Solids*, 2000, **278**, 75–84.
7. Mac Farlane, D. R., Javorniczky, J., Newman, P. J. and Booth, D. J., Enhanced fluorescence from nano-crystallized erbium-doped fluoroaluminate glasses. *J. Non-Cyst. Solids*, 1996, **1**(256/257), 366–371.
8. Coutier, C., Meffre, W., Jenouvrier, P., Fick, J., Audier, M., Rimet, R., Jacquier, B. and Langlet, M., The effect of phosphorous on the crystallization and photoluminescence behaviour of aerosol-gel deposited SiO_2–TiO_2–Er_2O_3–P_2O_5 thin films. *Thin Solid Films*, 2001, **392**, 40–49.
9. Coutier, C., Audier, M., Fick, J., Meffre, W., Rimet, R. and Langlet, M., Aerosol-gel preparation of ptically active layer in the system Er/SiO_2–TiO_2. *Thin Solid Films*, 2000, **372**, 177–189.
10. Strohhöfer, C., Fick, J., Vasconcelos, H. C. and Almeida, R. M., Active optical properties of Er-containing crystallites in sol–gel derived glass films. *J. Non-Cyst. Solids*, 1988, **226**, 182–191.
11. Tick, P. A., Borrelli, N. F. and Reaney, I. M., The relationship between structure and transparency in glass-ceramic materials. *Opt. Mater.*, 2000, **15**, 81–91.
12. Riello, P., Canton, P., Comelato, N., Polizzi, S., Verità, M., Fagherazzi, G., Hofmeister, H. and Hopfe, S., Nucleation and crystallization behavior of glass-ceramic materials in the Li_2O–Al_2O_3–SiO_2 system of interest for their transparency properties. *J. Non-Cyst. Solids*, 2001, **288**, 127–139.
13. Lin, M.-H. and Wang, M.-C., Phase transformation and characterization of TiO_2 and ZrO_2 addition in the Li_2O–Al_2O_3–SiO_2 gels. *J. Mater. Res.*, 1996, **11**, 2611–2615.
14. Wang, M.-C., Lin, M.-H. and Liu, H.-S., Effect of TiO_2 addition on the preparation of beta-spodumene powders by sol–gel process. *J. Mater. Res.*, 1999, **14**, 196–203.
15. M.-C. Wang, N.-C. Wu, S. Yang, S.-B. Wen, *Metall. Mater. Trans. A: Phys. Metall. Mater. Sci.* 33A (2002) 171–181.
16. Boccaccini, A. R., Stumpfe, W., Taplin, D. M. R. and Ponton, C. B., Densification and crystallization of glass powder compacts during constant heating rate sintering. *Mater. Sci. Eng. A*, 2001, **219**, 26–31.
17. Eftekhari Yekta, B. and Marghussian, V. K., Sintering of β.q.SS and gahnite glass ceramics. *J. Eur. Ceram. Soc.*, 1999, **19**, 2963–2968.
18. Sung, Y.-M., Mechanical properties of cordierite and spodumene glass-ceramics prepared by sintering and crystallization heat treatments. *Ceram. Int.*, 1993, **23**, 401–407.
19. Wang, M.-C., Wu, N.-C., Yang, S. and Wen, S.-B., Morphology and microstructure in the sintering of β-spodumene precursor powders with TiO_2 additive. *J. Eur. Soc.*, 2003, **23**, 437–443.
20. Wang, M.-C., Yang, S., Wen, S.-B. and Wu, N.-C., Sintering Li_2O–Al_2O_3–$4SiO_2$ precursor powders with ultrafine TiO_2 additives. *Mater. Chem. Phys.*, 2002, **76**, 162–170.
21. Reisfeld, R., Zelner, M. and Patra, A., Fluorescence study of zirconia films doped by Eu^{3+}, Tb^{3+}, and Sm^{3+} and their comparison with silica films. *J. Alloys Comp.*, 2000, **300–301**, 147–151.
22. Tokita, M., Trends in advanced SPS spark plasma sintering systems and technology. *J. Soc. Powder Technol. Jpn.*, 1993, **30**, 790–804.
23. Shen, Z., Zhao, Z., Peng, H. and Nygren, M., Formation of tough interlocking microstructures in silicon nitride ceramics by dynamic ripening. *Nature*, 2002, **417**, 266–269.
24. Omori, M., Sintering, consolidation, reaction and crystal growth by the spark plasma system (SPS). *Mater. Sci. Eng.*, 2000, **A287**, 183–188.
25. Riello, P., Fagherazzi, G., Clemente, D. and Canton, P., X-ray Rietveld analysis with a physically based background. *J. Appl. Crystallogr.*, 1995, **28**(2), 115–120.
26. Riello, P., Canton, P. and Fagherazzi, G., Quantitative phase analysis in semicrystalline materials using the Rietveld method. *J. Appl. Crystallogr.*, 1998, **31**(1), 78–82.
27. Nakagawa, K. and Izumitani, T., Metastable phase separation and crystallization of Li_2O–Al_2O_3–SiO_2 glasses: determination of the miscibility gap from the lattice parameter of the precipitated β-quartz solid solution. *J. Non-Cyst. Solids*, 1972, **7**, 168–180.